Supplemental Information

Oxidative stress impairs cell death by repressing the nuclease activity of mitochondrial Endonuclease G

This file contains:

Supplementary Experimental Procedures

Supplementary Tables S1-S4

Supplementary Figures S1-S4

Supplementary Experimental Procedures

Protein expression and purification

All of the mutant CPS-6 and WAH-1 constructs were generated by the Quick-change Site-Directed Mutagenesis Kit (Stratagene). The cDNA corresponding to CPS-6 and WAH-1 was cloned into pRSFDuet and pET21b (Novagen), respectively, followed by co-transformation into BL21b (RIPL) for bacterial co-expression. The metal ion affinity chromatography-purified recombinant WAH-1, CPS-6 and CPS-6 mutants were dialyzed with the following buffer: 50 mM Tris-HCl pH 7.4 and 200 mM NaCl supplemented with either 2.5 mM DTT or 5 mM reduced L-glutathione as the reducing buffer or 0.25 mM or 2.5 mM H_2O_2 as the oxidizing buffer at 4ºC for 0 to 72 hours. The oxidizing buffer was replenished every 16 hours. The dialyzed protein samples were concentrated prior to size exclusion analyses. The WAH-1 protein samples were resolved by Superdex-200, and the sizes of the 2 ml fractions eluted from 57 to 85 ml were further analyzed by SDS-PAGE with Coomassie blue staining. CPS-6(H148A) and CPS-6(H148A/K131D/F132N) protein samples were resolved by Superdex-75, and the sizes of 2 ml fractions eluted from 51 to 75 ml were further analyzed by SDS-PAGE with Coomassie blue staining. The intensities of the Coomassie blue-stained polypeptide bands were quantified by scanning using AlphaEaseFC^{TM} software (Alpha Innotech Corporation).

Protein crystallization

Crystals of CPS-6(H148A/Q130K) were grown by the hanging-drop vapor diffusion method at 4ºC. The crystallization drop was made by mixing 0.5 µl of protein solution and 0.5 µl of reservoir solution. CPS-6(H148A/Q130K) (10 mg/ml) in buffer containing 50 mM Tris-HCl, pH 7.4, 200 mM NaCl and 2.5 mM DTT was crystallized using a reservoir solution containing 0.1 M sodium citrate tribasic dihydrate (pH 5.5) and 18% PEG 3350. Diffraction data were collected with the BL15A beamline at NSRRC, Hsinchu, Taiwan, and were processed and scaled by HKL2000. All diffraction statistics are listed in Table S3. The crystal structure of CPS-6(H148A/Q130K) was solved by the molecular replacement method using the crystal structure of CPS-6(H148A) (PDB ID: 3S5B) as the search model using the program MOLREP of CCP4. The models were built by Coot and refined by Phenix. The buried surface area values for the dimeric interfacial residues of CPS-6(H148A) and CPS-6(H148A/Q130K) were determined by the "Protein interfaces, surfaces and

assemblies" service PISA at the European Bioinformatics Institute (Krissinel and Henrick, 2007). The atomic coordinates for the CPS-6(H148A/Q130K) crystal structure reported in this paper have been deposited in the RCSB Protein Data Bank with the accession number 4QN0.

Tandem mass spectrometry

Both reduced and oxidized CPS-6 H148A proteins were digested by trypsin in 50 mM ammonium bicarbonate, pH 8.0 and 10% acetonitrile at 37ºC overnight with an enzyme-to-protein molar ratio of 1:50. The digested protein samples were desalted by C18 Zip-Tip prior to mass spectrometric analyses. CPS-6(H148A) tryptic peptide samples were reconstituted in buffer A (0.1% formic acid in H_2O) and analyzed on Waters Synapt G2 HDMS (Waters, Milford, MA). Samples were injected onto a 2 cm × 180 μm capillary trap column and separated on a 75 μm × 25 cm nanoACQUITY 1.7 μm BEH C18 column using a nanoACQUITY Ultra-Performance LC system (Waters, Milford, MA). The column was maintained at 35°C and bound peptides were eluted with a gradient of 5-40 % buffer B (0.1% formic acid in acetonitrile) for 30 min. Mass spectrometry (MS) was conducted in ESI positive V mode with a resolving power of 10000 and calibrated with a synthetic human [Glu1]-fibrinopeptide B solution (0.5 pmol/mL, Sigma-Aldrich) delivered through the NanoLockSpray source. Data acquisition was performed using the data directed analysis (DDA) method. The DDA method included one full MS scan (m/z 350-1600, 1 s/scan) and three MS/MS scans (m/z 100-2000, 1 s/scan) performed sequentially on the three most intense ions present in the full scan mass spectrum. The MS and MS/MS raw data were converted into peak lists using ProteinLynx Global Server 2.5 (Waters, Milford, MA). Analysis of all MS/MS samples was performed using Mascot (Matrix Science; version 2.4.0). Mascot was set up to search an in-house-generated database, assuming trypsin as the digestion enzyme. A database search against Mascot was performed with a fragment ion mass tolerance of 0.05 Da and a parent ion tolerance of 25 ppm. Two missed cleavages were allowed during trypsin digestion. Oxidation of D, F, K, M, N, P, Y, H and W were respectively specified as variable modifications. Oxidation sites and peptide sequence assignments contained in MASCOT search results were validated by manual confirmation from raw MS/MS data.

The reduced or oxidized WAH-1 proteins (10 μM) were incubated with thermolysin (0.6 μM) at 65°C overnight in 50 mM phosphate buffer pH 6.0 and 0.5

mM $CaCl_2$. The digested samples were desalted by C18 Zip-Tip prior to tandem mass spectrometric analyses. NanoLC-nanoESi-MS/MS analysis was performed on a nanoAcquity system (Waters, Milford, MA, USA) connected to an LTQ-Orbitrap XL hybrid mass spectrometer (Thermo Fisher Scientific, Bremen, Germany) equipped with a nanospray interface (Proxeon, Odense, Denmark). Either reduced or oxidized WAH-1 thermolysin peptide mixtures were loaded onto a 75 μm ID, 25 cm length C18 BEH column (Waters, Milford, MA, USA) packed with 1.7 μm particles with a pore width of 130 Å and were separated using a segmented gradient from 5% to 40% solvent B (acetonitrile with 0.1% formic acid) at a flow rate of 300 nl/min for 60 min and a column temperature of 35°C. Solvent A was 0.1% formic acid in water. MS was conducted in the data-dependent mode. Briefly, full scan MS spectra were acquired in the orbitrap (*m/z* 350–1600) with the resolution set to 60,000 at *m/z* 400 and an automatic gain control (AGC) target of 10^6. The 10 most intense ions were sequentially isolated for CID MS/MS fragmentation and detection in the linear ion trap (AGC target at 7000), with previously selected ions dynamically excluded for 90 s. Ions with single and unrecognized charge states were also excluded. All the measurements in the orbitrap were performed with the lock mass option for internal calibration. The cross-linked cysteine residues are listed in Tables S1 and S2. The scores were generated by MassMatrix (http://www.massmatrix.net/xmapper) using a previously-described algorithm (Xu and Freitas, 2007; Xu et al., 2010).

Circular dichroism (CD) spectrometry

The CD spectra of either CPS-6(H148A) or CPS-6(H148A/Q130K) at a concentration of 10 μM were recorded at 25ºC on an AVIV 62DS CD spectrometer (Lakewood, NJ, USA). The CD spectra were measured in the range of 195 to 250 nm using a quartz cell with a light path of 1 mm. The spectra were recorded as the average of 5 scans for each recombinant protein sample after correction for the baseline contribution of buffer. The data are reported as the mean residue molar ellipticities ([θ]). The melting points (Tm) of CPS-6(H148A) and CPS-6(H148A/Q130K) at a concentration of 10 μM were measured by CD at a wavelength 205 nm from 10-90ºC. The Tm values were determined by the first derivative of the CD transition curves.

Intrinsic tryptophan emission fluorescence spectrometry

Intrinsic tryptophan fluorescence was measured using a Varian Cary Eclipse

Fluorescence Spectrophotometer (Agilent Technologies) at 25ºC. The intrinsic fluorescence of the multiple tryptophan residues Trp^{99} and Trp^{184} of CPS-6(H148A) and Trp^{288}, Trp^{289}, Trp^{543}, Trp^{564} and Trp^{593} of WAH-1 were used to monitor the solution structures of the proteins. Spectra were obtained using an excitation wavelength of 296 nm and performing emission scans at 0.5 nm intervals between 300 to 500 nm. The slit widths for the excitation and emission monochrometers were 5 and 10 nm, respectively. The CPS-6 and WAH-1 binding signal, *F*, was obtained by the following equation:

$$F = F_{bound\ CPS\text{-}6} - F_{free\ CPS\text{-}6}$$

where $F_{bound\ CPS\text{-}6}$ is the intrinsic tryptophan fluorescence intensity after the addition of CPS-6 in the presence of 65 nM WAH-1 and $F_{free\ CPS\text{-}6}$ is the intrinsic tryptophan fluorescence of free CPS-6 at λ_{max}=341nm.

The CPS-6 and WAH-1 binding curve (equilibrium type) was analyzed using the non-linear regression program GraphPad Prism 4 (GraphPad Inc.), whereby two linear segments were drawn based upon the best-fit curve to determine the protein-protein binding molar ratio (Groemping and Hellmann, 2005). For simple rectangular hyperbolic CPS-6 and WAH-1 interaction, the binding function can be defined as r = f_a x p, where p is the number of CPS-6 binding sites on WAH-1 and f_a is the fractional saturation that was determined as:

$$f_a \text{ (fraction of CPS-6 binding site occupied on WAH-1)} = (1-F/F_o)/[1-(F/F_o)^*]$$

where F is the binding signal after the addition of CPS-6 and F_o is the binding signal before the addition of CPS-6 at λ_{max}=341nm, respectively. The protein-protein saturation $(F/F_o)^*$ value was determined at 10 μM CPS-6 where the binding curve reached a plateau. At equilibrium, the protein-protein interaction can be described as:

$$r/\boldsymbol{C}_S = pK_a - rK_a$$

The K_a (K_d) values were calculated from the slope of the plot of r/Cs μM^{-1} versus r (Groemping and Hellmann, 2005).

Nuclease activity assays

The recombinant CPS-6 was incubated with 2.5 mM DTT or 2.5 mM H_2O_2 at 4°C for 16 hours to generate the reduced or oxidized forms of CPS-6, respectively. For the DNase activity assays shown in Figure 2 (the eluted oxidized protein fractions collected from S-75), CPS-6 enzymes were incubated with 25 ng pET28 plasmid DNA in 50 mM Tris-HCl pH7.4, 200 mM NaCl, 2 mM $MgCl_2$ and 2.5 mM DTT at

37ºC for 60 min. For the plasmid nicking assays shown in Figure 2, the reduced or oxidized wild-type CPS-6 at a concentration of 0.5 μM was incubated with 12.5 ng pET28 plasmid DNA in the presence of either the reducing buffer A (10 mM HEPES pH7.0, 40 mM NaCl, 2 mM $MgCl_2$ and 2 mM DTT) or the oxidizing buffer B (10 mM HEPES pH7.0, 40 mM NaCl, 2 mM $MgCl_2$ and 2 mM H_2O_2) at 37ºC for 30 min.

For the DNase activity assays shown in Figure 3C, 25 ng of pET28 plasmid DNA was incubated with 1 μM CPS-6 with or without the addition of 2 μM WAH-1 in the presence of either reducing buffer A or oxidizing buffer B at 37ºC for 25 minutes. For the DNase activity assays shown in Figure 3D, 25 ng of pET28 plasmid DNA was incubated with 1 μM CPS-6 and/or 2 μM WAH-1 (either in reduced monomeric or oxidized dimeric form) in the presence of oxidizing buffer A at 37ºC for 15 min.

For Figure 4A, 25 ng of pET28 plasmid DNA was incubated with 2 μM purified CPS-6 or CPS-6(Q130K) mutant in the presence of the reduced buffer A at 37ºC for 35 min. All the digested DNA samples were resolved on a 1% agarose gel, stained by ethidium bromide, and detected with a charge-coupled device camera at UV trans-illumination. The intensity of undigested supercoiled DNA was quantified by the software AlphaEaseFC (version 4.0.0) (Alpha Innotech) to calculate the percentage of digested plasmid DNA.

In vivo cell death assays in C. elegans

A $P_{dpy\text{-}30}$CPS-6 construct was used for *in vivo* expression of CPS-6 (Parrish and Xue, 2003). To construct $P_{dpy\text{-}30}$CPS-6(Q130K), $P_{dpy\text{-}30}$CPS-6 was used as a DNA template to make the indicated amino acid substitutions using a Quick Change mutagenesis kit (Stratagene). $P_{dpy\text{-}30}$WAH-1 was constructed by subcloning 2103 bp *wah-1* cDNA into the pS235 vector via its Nhe I and Sal I sites. *C. elegans* strains were maintained using standard procedures (Brenner, 1974). The CPS-6 expression constructs were injected at 20 μg/ml into *cps-6(sm116)* or *wah-1(tm1159)/*hT2(*qIs48*) animals as previously described (Mello et al., 1991), using the pTG96 plasmid at 20 μg/ml as a co-injection marker that directs GFP expression in all cells in most developmental stages (Gu et al., 1998). The $P_{dpy\text{-}30}$WAH-1 constructs were injected at 1 μg/ml into N2 animals with the pTG96 plasmid at 20 μg/ml as a co-injection marker. The transgenic arrays were then crossed into *wah-1(tm1159)/*hT2(*qIs48*) animals for phenotypic analysis. The numbers of cell corpses in living embryos at different

embryonic stages were scored using Nomarski optics as described previously (Parrish and Xue, 2003). *wah-1(tm1159)* homozygous embryos were identified as embryos that lost the hT2(*qIs48*) balancer and did not show any pharyngeal GFP expression derived from *qIs48*. To treat animals with paraquat (Sigma-Aldrich) or reduced glutathione (Sigma-Aldrich), paraquat or reduced glutathione dissolved in 100 μl water was added to 5 ml NGM agar plates and incubated for 3 minutes to allow absorption of the chemical by NGM media. One hundred L4 animals were placed on the plates and incubated overnight to let them lay eggs, which were then scored for cell corpses.

Co-immunoprecipitation assays in C. elegans

The $P_{dpy\text{-}30}$CPS-6::GFP construct was injected at 20 μg/ml into *cps-6(sm307)* animals, which contain a *cps-6::flag* knockin in their genome generated by the CRISPR/Cas9 gene editing technique (Zhao et al., 2014). pRF4 plasmid was used at 20 μg/ml as a co-injection marker, which causes a Roller phenotype. Transgenic animals were incubated with or without 200 μM paraquat on NGM plates for 3 days. Five hundred transgenic L4 animals were harvested. Sonication, co-immunoprecipitation experiments, SDS-PAGE and immunoblotting were performed as described previously (Geng et al., 2008), using anti-Flag M2 affinity beads (Sigma). For immunoblotting, we used a rat anti-GFP antibody (Life Technologies, catalog# A11122) as a primary antibody at 1:3,000 dilution and goat anti-rat IgG HRP (Abcam, catalog# ab97057) as a secondary antibody at 1:10,000 dilution. The signal intensities were measured using ImageJ as previously described (Nakagawa et al., 2014).

Statistical methods

The P values presented in Figure 2C and Figure 4A were estimated by the Student's t-test for paired samples using Microsoft Excel® (USA). When P value is greater than 0.05, the difference between two sets of experimental data was deemed as insignificant. In Figure S4D, the CPS-6 and WAH-1 binding points were fitted by non-linear regression performed by GraphPad Prism 4 (GraphPad Software USA). In Figure S4E, the standard error generated for the dissociation constant, Kd, was calculated by three independent experiments via GraphPad Prism 4 (GraphPad Software USA).

References

Brenner, S. (1974). The genetics of *Caenorhabditis elegans*. Genetics *77*, 71-94.

Geng, X., Shi, Y., Nakagawa, A., Yoshina, S., Mitani, S., Shi, Y., and Xue, D. (2008). Inhibition of CED-3 zymogen activation and apoptosis in *Caenorhabditis elegans* by caspase homolog CSP-3. Nat. Struct. Mol. Biol. *15*, 1094 - 1101.

Groemping, Y., and Hellmann, N. (2005). Current Protocols in Protein Science. John Wiley & Sons, Inc., 20.28.21-20.28.27.

Gu, T., Orita, S., and Han, M. (1998). *Caenorhabditis elegans* SUR-5, a novel but conserved protein, negatively regulates LET-60 Ras activity during vulval induction. Mol. Cell. Biol. *18*, 4556–4564.

Krissinel, E., and Henrick, K. (2007). Inference of macromolecular assemblies from crystalline state. J. Mol. Biol. *372*, 774--797.

Mello, C.C., Krame, J.M., Stinchcomb, D., and Ambros, V. (1991). Efficient gene transfer in *C. elegans*: Extrachromosomal maintenance and integration of transforming sequences. EMBO J. *10* 3959-3970.

Nakagawa, A., Sullivan, K.D., and Xue, D. (2014). Caspase-activated phosphoinositide binding by CNT-1 promotes apoptosis by inhibiting the AKT pathway Nat. Struct. Mol. Biol. *21*, 1082-1090.

Parrish, J.Z., and Xue, D. (2003). Functional genomic analysis of apoptotic DNA degradation in *C. elegans*. Mol. Cell *11*, 987-996.

Xu, H., and Freitas, M.A. (2007). A mass accuracy sensitive probability based scoring algorithm for database searching of tandem mass spectrometry data. BMC Bioinfor. *8*, 133.

Xu, H., Hsu, P.H., Zhang, L., Tsai, M.D., and Freitas, M.A. (2010). Database search algorithm for identification of intact cross-links in proteins and peptides using tandem mass spectrometry. J. Proteome Res *9*, 3384-3393.

Zhao, P., Zhang, Z., Ke, H., Yue, Y., and Xue, D. (2014). Oligonucleotide-based targeted gene editing in C. elegans via the CRISPR/Cas9 system. Cell Res. *24*, 247-250.

Table S1. Identification of the oxidized amino acids in oxidized CPS-6(H148A) by LC-MS/MS, related to Figure 2.

m/z (Dalton) Reduced CPS-6*	m/z (Dalton) Oxidized CPS-6*	CPS-6 H148A tryptic fragments[#]	Oxidized CPS-6 amino acid(s)	LC MS/MS spectra
1146.57	1162.54	^{72}HGYPG**F**TNVR^{81}	F77[&]	Figure S2C
1850.05	1882.03	^{197}K**M**INSYIITG**P**LYLPK^{212}	M198, P207[&]	Figure 2D

*: The monoisotopic mass (Da) values were obtained empirically.

[#]: Oxidized amino acids identified from oxidized CPS-6(H148A) tryptic fragments are shown in bold and underlined.

[&]: Interfacial amino acids identified from dimeric CPS-6(H148A)(PDB: 3S5B).

Table S2. Identification of the oxidized amino acids in the thermolysin fragments of the disulfide-linked WAH-1 dimer, related to Figure 3.

m/z (Dalton) * Oxidized WAH-1	pp& value	Oxidized WAH-1 dimer thermolysin fragments#	Crosslinked WAH-1 Cys residues	LC MS/MS spectra
1865.9130	13.2	^{237}LLH**C**EY^{242} and ^{342}VKI**C**EEDKK^{350}	Cys240 and Cys345	Figure S3
1824.8722	18.1	^{344}I**C**EEDKKV^{351} and ^{344}I**C**EEDKK^{350}	Cys345 and Cys345	Figure S3
1552.7478	17.7	^{344}I**C**EEDKK^{350} and ^{530}VRADK**C**^{535}	Cys345 and Cys535	Figure S3

*: The monoisotopic mass values were obtained empirically.

&: The pp value is the major standard used in MassMatrix, and the peptide matches with pp value greater than 6 are considered to be statistically significant.

#: Disulfide-bond forming cysteine residues identified from thermolysin fragments of oxidized WAH-1 are labeled in bold and underlined.

Table S3. Disulfide bonds mapped by tandem mass spectrometric analyses and subsequent database search in MassMatrix for the digested samples, related to Figure 3.

‡Reduced WAH-1

	C240	C345	C484	C485	C535	C614
C240	0	0	0	0	0	0
C345	0	0	3.7	0	0	0
C484	0	3.7	0	0	0	0
C485	0	0	0	0	3.7	0
C535	0	0	0	3.7	4.1	0
C614	0	0	0	0	0	0

‡ Oxidized WAH-1 (monomer)

	*C240	*C345	C484	C485	*C535	C614
*C240	33.3	**178.9**	32.1	52.7	66.0	83.2
*C345	**178.9**	23.2	64.4	14.7	**128.4**	77.6
C484	32.1	64.4	0	3.4	31.6	38.7
C485	52.7	14.7	3.4	4.5	20.1	27.9
*C535	66	**128.4**	31.6	20.1	0	42.8
C614	83.2	77.6	38.7	27.9	42.8	6.3

‡Oxidized WAH-1 (dimer)

	*C240	*C345	C484	C485	*C535	C614
*C240	13.4	**164.2**	40.8	49.3	35.9	63.4
*C345	**164.2**	**159.2**	42.8	50.5	**178.9**	98.7
C484	40.8	42.8	0	0	32.6	56
C485	49.3	50.5	0	0	23.3	7.3
*C535	35.9	**178.9**	32.6	23.3	0	54
C614	63.4	98.7	56	7.3	54	19.2

‡: The crosslink scores between cysteine residues were generated from MassMatrix (http://www.massmatrix.net/xmapper) based on the algorithm described previously (*33, 34*). The values listed in the Reduced WAH-1 and Oxidized WAH-1 (monomer) are normalized to the Oxidized WAH-1 (dimer).
***:** predominant disulfide bond forming cysteine residues.

Table S4. Crystallographic statistics of CPS-6 H148A/Q130K, related to Figure 4.

Data collection and processing	**Values**
Wavelength (Å)	1.0
Space group	$P2_1$
Cell dimensions (a, b, c/ β) (Å/ degree)	67.6, 122.6, 73.6/ 96.0
Resolution (Å)	50.0-2.75 (2.80-2.75)*
Observed/unique reflections	116,064/31,165
Data redundancy	3.7 (3.8)
Completeness (%)	99.7 (100)
R_{sym} (%)	7.7 (44.5)
$I/\sigma(I)$	14.0 (3.3)
Refinement statistics	
Resolution range	26.49 - 2.74
Reflections (work/test)	29,535/1,965
R-factor/R-free (%)	18.5/23.5
Number of non-hydrogen atoms-	
Protein/metal ions/water molecules	7,682/4/179
Model quality	
RMSD in bond length (Å)/bond angle (^{o})	0.005/0.927
Average B-factor-	
protein/metal/solvent ($Å^2$)	25.1/27.3/26.4
Ramachandran plot-	
Most favored	96.7
Additionally allowed	3.3
Generally allowed and disallowed	0.0

*Values in parentheses refer to the highest resolution shell.

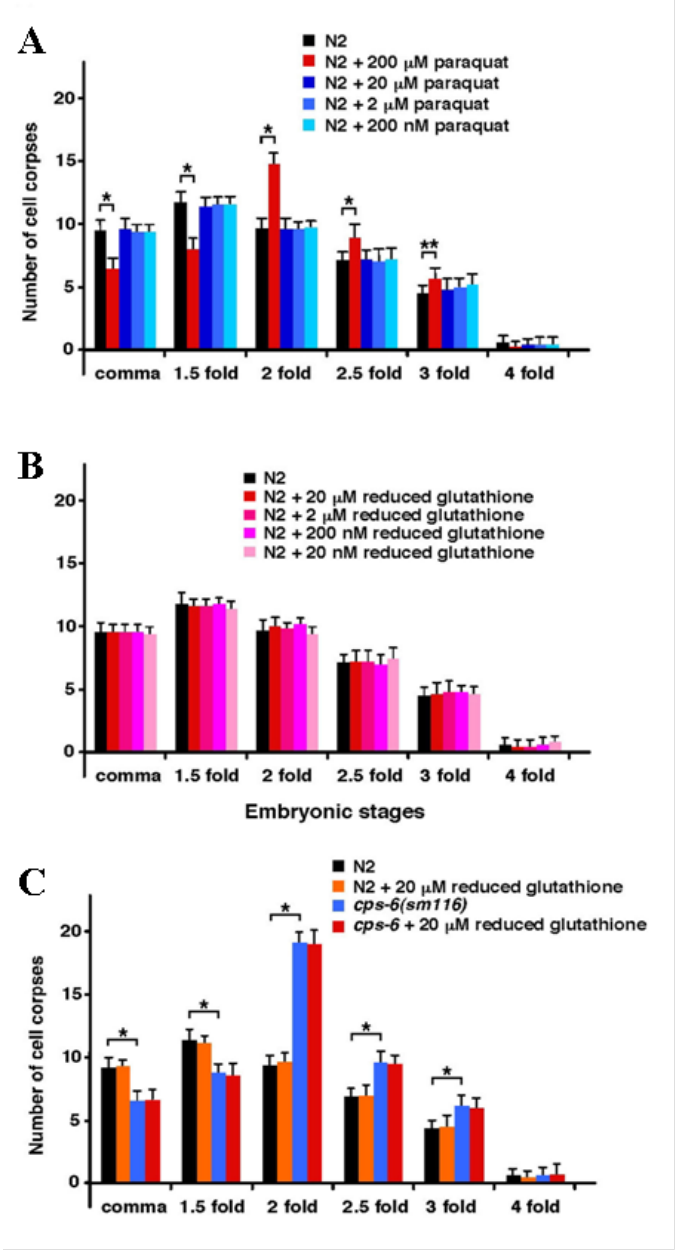

Figure S1, related to Figure 1. The effects of oxidative or reduced conditions on cell death in *C. elegans*. Embryonic cell corpses were scored from the indicated strains in the presence of paraquat or reduced glutathione at the indicated concentrations. (A) N2 animals were exposed to 200 μM, 20 μM, 2 μM, or 200 nM of paraquat. (B) N2 animals were exposed to 20 μM, 2 μM, or 200 nM or 20 nM of reduced glutathione. (C) Reduced glutathione did not alter the cell corpse profiles of N2 or *cps-6(sm116)* animals. Stages of embryos examined were comma, 1.5-fold, 2-fold, 2.5-fold, 3-fold and 4-fold. The *y*-axis represents the mean of cell corpses scored in embryos (n=15), and error bars represent the standard deviation (SD). The significance of differences were determined by two-way ANOVA, followed by Bonferroni comparison. *, $P < 0.001$; **, $P < 0.05$. All other points had P values > 0.05.

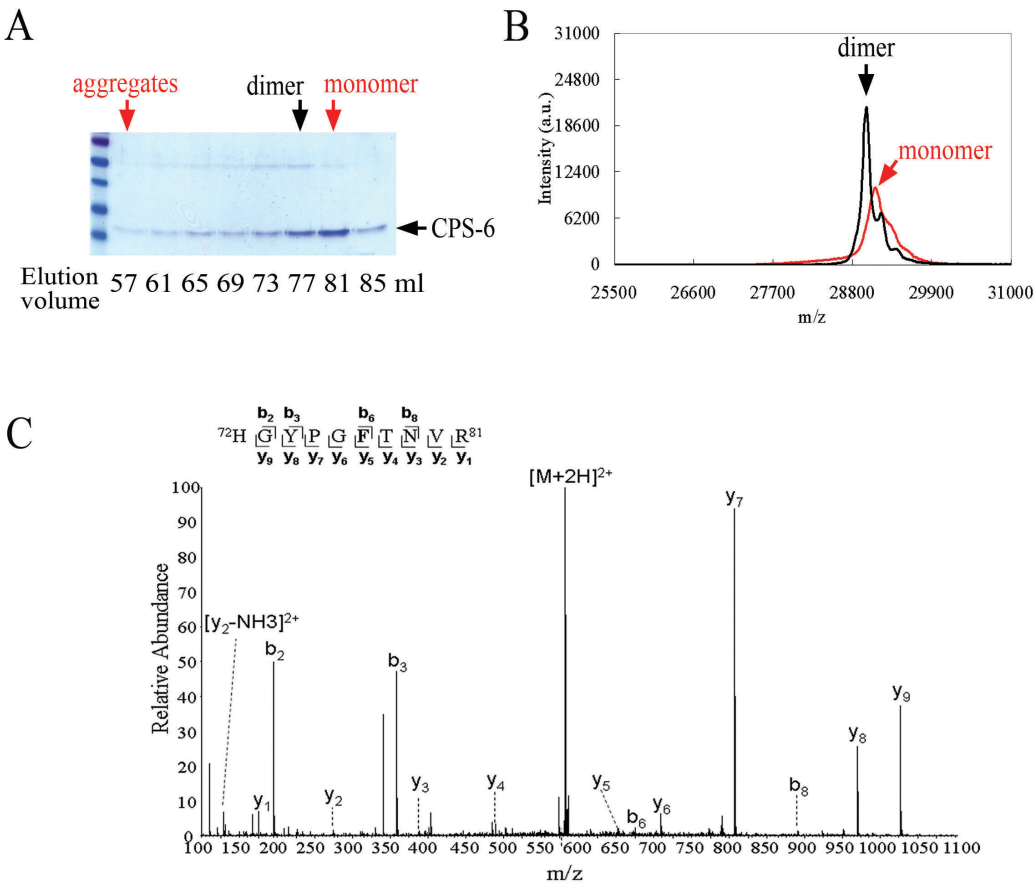

Figure S2, related to Figure 2. The estimated molecular weights of CPS-6 under reduced and oxidized conditions. (A) After incubation with H_2O_2, CPS-6 was fractionated by size exclusion chromatography (Superdex 200), and all the protein fractions were analyzed by SDS-PAGE showing that CPS-6 in the aggregated, dimeric and monomeric fractions was intact and not degraded. (B) The estimated molecular weight (MW) of the reduced CPS-6 was 29,001 Dalton, whereas the estimated MW of the oxidized CPS-6 was 29,116 Dalton as measured by MASS spectrometry (calculated MW of CPS-6 is 28,947 Dalton). The molecular weight of the oxidized CPS-6(H148A) was increased by 115 Dalton as compared to the reduced CPS-6. The intensity of the mass spectrometry is represented by a.u. (arbitrary unit). (C) Representative MS/MS spectrum obtained for the predominant trypsin fragment of the oxidized CPS-6: His72-Arg81, showing that F77 was oxidized. The fragments and oxidized residues F77, M198 and P207 are listed in Table S1.

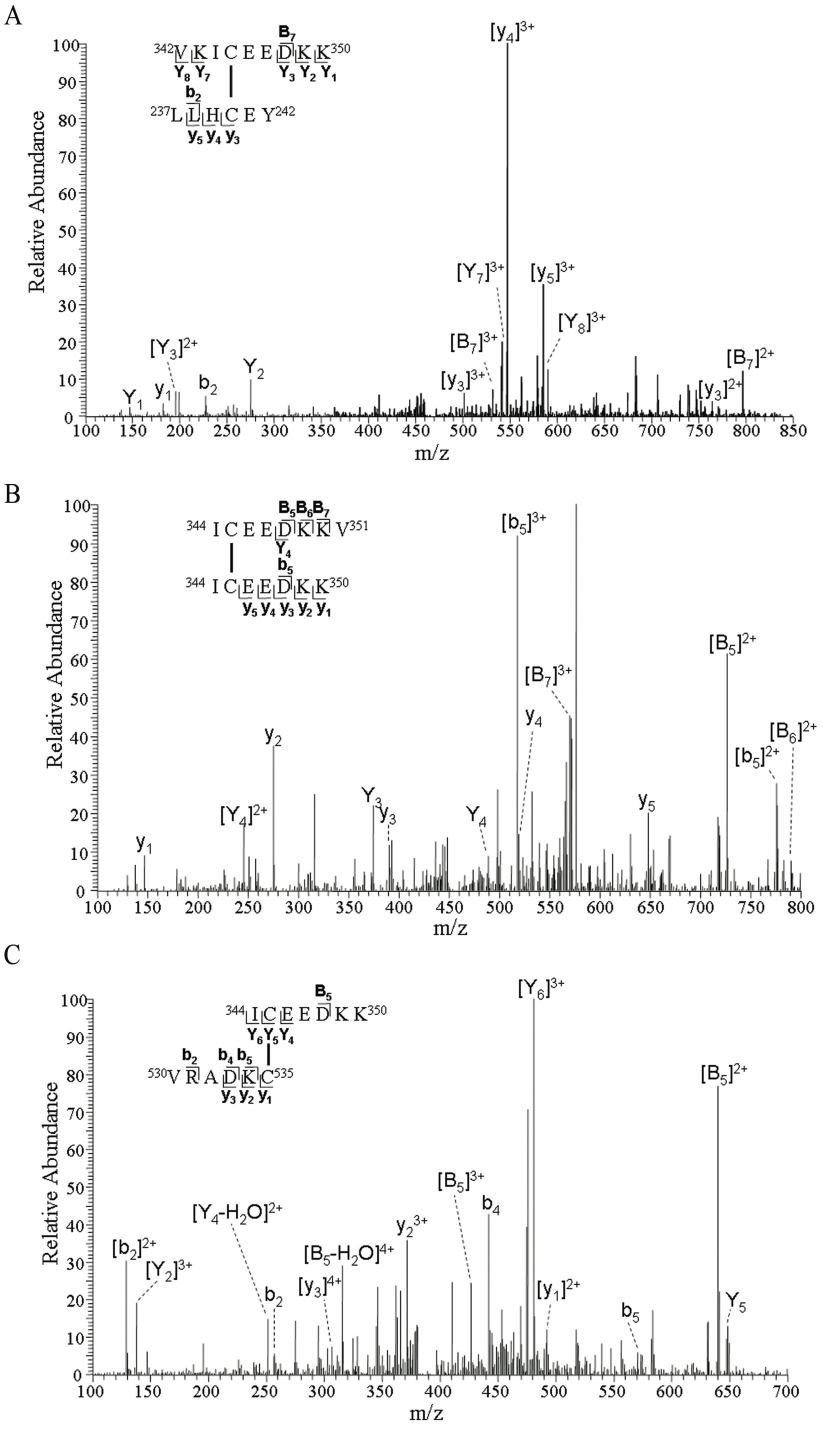

Figure S3, related to Figure 3. Representative MS/MS spectra obtained for three predominant thermolysin fragments of the disulfide-linked WAH-1 dimer. The fragments are listed in Table S2.

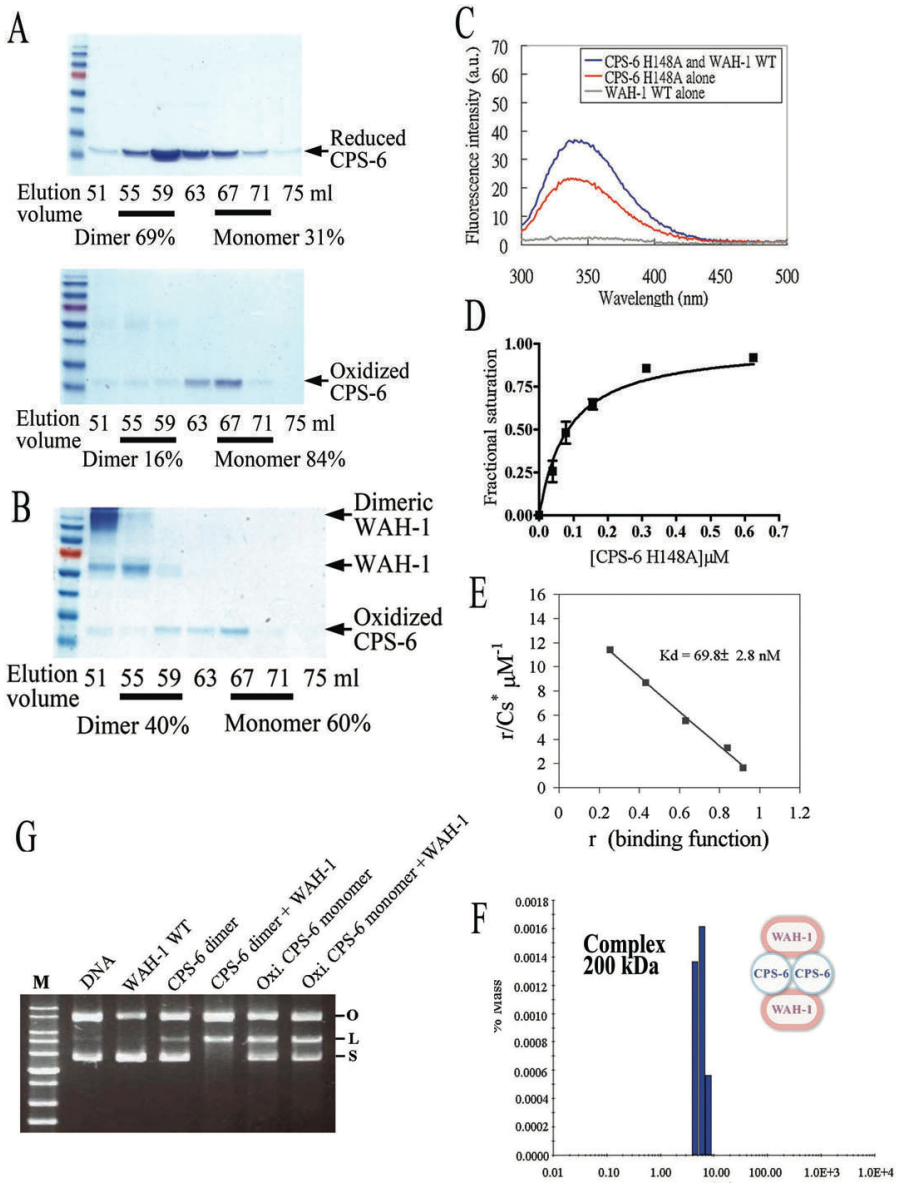

Figure S4, related to Figure 3. WAH-1 interacts with CPS-6 to enhance the stability and nuclease activity of dimeric CPS-6. (A) The dimer/monomer ratio of the reduced and oxidized CPS-6(H148A) eluted from S-75 chromatography as analyzed by SDS-PAGE. (B) The CPS-6 dimer percentage was significantly higher in the presence of wild-type WAH-1 under oxidative conditions. (C) Intrinsic fluorescence spectrometry was performed to monitor CPS-6(H148A) and WAH-1 interactions at an emission maximum wavelength λ_{max}=347 nm. (D) The protein-protein binding signals were converted into fractional saturation values. (E) The CPS-6 to WAH-1 molar ratio was estimated to be 1:1 as extrapolated from binding curves. The Kd value was 69.8 ± 2.8 nM as calculated by Scatchard analyses. The Cs* value represents the unbound concentration of CPS-6 H148A. (F) CPS-6 and WAH-1 eluted as a complex in the size exclusion chromatography (S200) in the absence of DTT. This complex had a molecular mass of about 200 kDa, as measured by DLS. (G) WAH-1 only enhanced the nuclease activity of the purified dimeric CPS-6, but not that of the oxidized monomeric CPS-6.